JOURNAL OF THEORETICAL
AND APPLIED MECHANICS
1, 37, 1999

DYNAMIC BEHAVIOUR OF AN AXIALLY MOVING THIN ORTHOTROPIC PLATE

KRZYSZTOF MARYNOWSKI

Department of Machines Dynamics, Technical University of Łódź
email: kmarynow@ck-sg.p.lodz.pl

ZBIGNIEW KOŁAKOWSKI

Department of Strength Materials and Structures, Technical University of Łódź
email: kola@orion.p.lodz.pl

A new approach to analysis of the dynamic behaviour of axially moving orthotropic plates is presented. The nonlinear orthotropic plate theory is modified to include the inertial forces resulting from the moving web. The results of numerical investigations show the solution to a linear problem. The effects of the orthotropy factor, axial transport velocity and rolls support system on transverse and torsional natural frequencies and stability of the plate motion are presented. The lowest natural frequencies decrease with the increasing axial velocity at undercritical transport speeds. The plate may experience divergent or flutter instability at supercritical transport speeds. A second stable region above the critical speed may exist as well.

Key words: moving plate, orthotropy, dynamic stability

Notation

b	–	width of the plate
c	–	axial transport speed
D	–	flexural stiffness of the plate
E_x, E_y	–	Young modulus of the plate along x and y axes, respectively
G	–	modulus of non-dilatational strain of the plate
h	–	thickness of the plate
J	–	number of the constituent plates

l	–	length of the plate
m	–	number of the natural frequency
K	–	total number of natural frequencies
M_{xi}, M_{yi}, M_{xyi}	–	bending moment resultants for the ith plate
N_{xi}, N_{yi}, N_{xyi}	–	inplane stress resultants for the ith plate
q_i	–	transverse loading of the ith plate
R	–	axial tension
T	–	function of time
t	–	time
u_i, v_i, w_i	–	displacement components of the ith plate middle surface
$\varepsilon_{xi}, \varepsilon_{yi}, \varepsilon_{xyi}$	–	strain tensor components for the middle surface of the ith plate
η	–	orthotropy factor of the plate, $\eta = E_y/E_x$
κ	–	equivalent stiffness of the rolls support structure
$\kappa_{xi}, \kappa_{yi}, \kappa_{xyi}$	–	curvature modifications and torsions of the middle surface of the ith plate
λ	–	scalar load parameter
ν_{xy}, ν_{yx}	–	Poisson ratio of the plate; the first index represents transverse direction and the second shows the load direction
ξ	–	nondimensional mode amplitude parameter
ρ_i	–	mass density of the ith plate
σ	–	real part of the eigenvalue
ω	–	natural frequency of the plate (imaginary part of the eigenvalue).

1. Introduction

The class of axially moving continua of thin flat rectangular shape material with small flexural stiffness, called a web, encompasses such systems as power transmission belts, magnetic tapes, band saws and paper tapes. Vibration characteristics and dynamic stability investigations of such systems are required for analysis and optimal design of technological devices.

A lot of the earlier works in this field focused on dynamic investigations of string-like and beam-like axially moving isotropic systems (e.g. Wickert and Mote, 1988, 1990). In the case of a two-dimensional axially moving thin plate, the exact dynamic solutions satisfying the non-linear coupled equations

governing the web motion, probably cannot be determined in a closed form. Recent works analysed the equilibrium displacement, stress distribution (Lin and Mote, 1995), wrinkling phenomenon (Lin and Mote, 1996) and stability of axially moving isotropic plate (Lin, 1997).

It is well known that many materials traditionally considered as isotropic exhibit some degree of anisotropy due to working processes. Also growing interest in composite materials demands a better understanding of the strength of materials anisotropic by design. The aim of this paper is to analyse the dynamic behaviour of axially moving orthotropic thin plate. A new approach to solving of this problem is proposed. To derive the equations of motion. the nonlinear thin-walled orthotropic plate theory is modified to include the inertial forces resulting from the plate motion. The differential equations of motion are derived from Hamilton's principle taking into account the Lagrange description, the strain Green tensor for thin-walled plates and the Kirchhoff stress tensor. The singular perturbation theory is used to obtain an approximate analytical solution of the governing equations. The numerical methods of Unger's transition matrix and Godunov's orthogonalization procedure are used to solve the eigenvalue and eigenvector problems.

One of the principal goals of numerical analysis is to investigate the effect of the orthotropy factor on dynamic behaviour of two different materials of the plate. Numerical results show the effects of axial velocity, rolls support system and orthotropy factors on the plate vibrations and stability.

2. Formulation of the structural problem

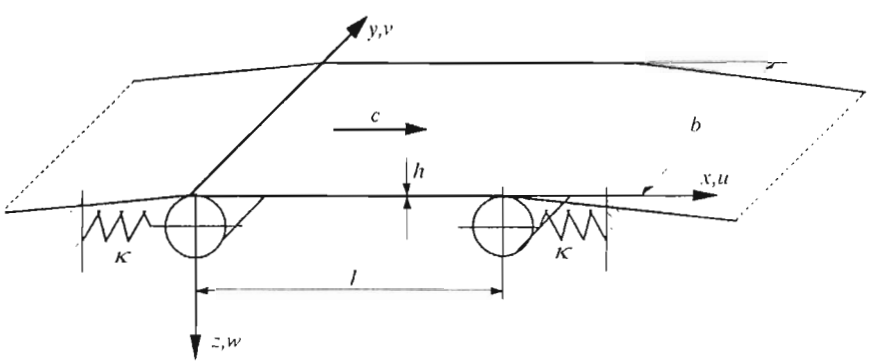

Fig. 1. Axially moving plate

A long elastic moving plate of the length l is considered. The plate coordinates and geometry are shown in Fig.1. The dynamic analysis is carried out using the thin-walled plate model. The considered web is composed of plane rectangular plate segments, the principal axes of orthotropy of which are parallel to their edges. Such a model allow for a dynamic analysis of plates with various material properties and parameters. These component plate segments are interconnected along the longitudinal edges. Basic geometrical dimensions of the structure are presented in Fig.2.

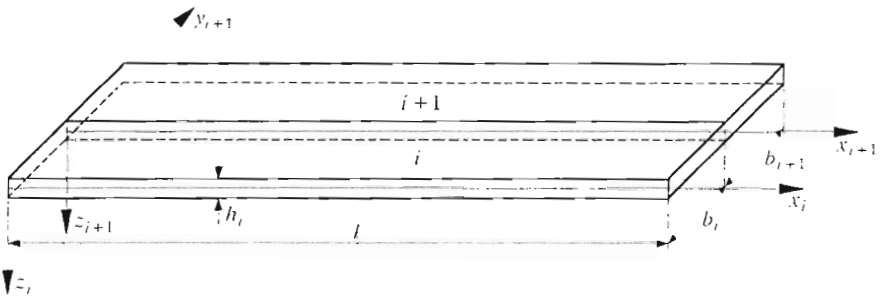

Fig. 2. Prismatic plate structure and the local co-ordinate system

The orthotropic materials of moving plate obey Hook's law. Because of significant transport velocities the elasto-plastic deformations and reologic phenomena have not been taken into account. For the ith plate the geometrical relationships in the Lagrange description are assumed taking into account both the out-of-plane and in-plane deformations (Chandra and Raju, 1973, Kołakowski and Królak, 1995)

$$\begin{aligned} &\varepsilon_{xi} = u_{i,x} + 0.5w_{i,x}^2 \qquad \varepsilon_{yi} = u_{i,y} + 0.5w_{i,y}^2 \\ &\gamma_{xyi} = 2\varepsilon_{xyi} = u_{i,y} + v_{i,x} + w_{i,x}w_{i,y} \\ &\kappa_{xi} = -w_{i,xx} \qquad \kappa_{yi} = -w_{i,yy} \qquad \kappa_{xyi} = -w_{i,xy} \end{aligned} \tag{2.1}$$

The dependence between the Young modulus and the Poisson ratio is as follows

$$E_{xi}\nu_{yxi} = E_{yi}\nu_{xyi} \tag{2.2}$$

The relationships between stresses and strains for the ith plate are formulated in the following way

$$N_{xi} = \frac{E_i h_i}{1-\eta_i \nu_i^2}(\varepsilon_{xi} + \eta_i \nu_i \varepsilon_{yi}) \qquad N_{yi} = \frac{E_i h_i \eta_i}{1-\eta_i \nu_i^2}(\varepsilon_{yi} + \nu_i \varepsilon_{xi})$$

$$N_{xyi} = G_i h_i \gamma_{xyi} = 2G_i h_i \varepsilon_{xyi} \qquad M_{xi} = -D_i(w_{i,xx} + \eta_i \nu_i w_{i,yy}) \tag{2.3}$$

$$M_{yi} = -\eta_i D_i(w_{i,yy} + \nu_i w_{i,xx}) \qquad M_{xyi} = -D_{1i} w_{i,xy}$$

where

$$E_i = E_{xi} \qquad \eta_i = \frac{E_{yi}}{E_{xi}} \qquad \nu_i = \nu_{xyi}$$
$$\nu_{yxi} = \eta_i \nu_i \qquad D_i = \frac{E_i h_i^3}{12(1-\eta_i \nu_i^2)} \qquad D_{1i} = \frac{G_i h_i^3}{6} \tag{2.4}$$

The differential equilibrium equations resulting from Hamilton's principle and the corresponding expressions appearing in Eqs (2.1) for the ith plate can be written as follows

$$\begin{aligned}
&\rho_i h_i(-u_{i,tt} - 2cu_{i,xt} - c^2 u_{i,xx}) + N_{xi,x} + N_{xyi,y} = 0\\
&\rho_i h_i(-v_{i,tt} - 2cv_{i,xt} - c^2 v_{i,xx}) + N_{xyi,x} + N_{yi,y} = 0\\
&\rho_i h_i(-w_{i,tt} - 2cw_{i,xt} - c^2 w_{i,xx}) + M_{xi,xx} + 2M_{xyi,xy} + M_{yi,yy} +\\
&+q_i + (N_{xi} w_{i,x})_{,x} + (N_{yi} w_{i,y})_{,y} + (N_{xyi} w_{i,x})_{,y} + (N_{xyi} w_{i,y})_{,x} = 0
\end{aligned} \tag{2.5}$$

The equations of Hamilton's principle are given in Appendix A. The kinematics and static continuity conditions at joint of adjacent plates are given in Appendix B.

The non-linear problem is solved by the asymptotic method. The displacement fields u_i, v_i, w_i are expanded into a power series with respect to ξ normalised by the equality condition of the maximum plate deflection and its thickness h_i

$$\begin{aligned}
u_i &= \lambda u_{0i} + \xi u_{1i} + \xi^2 u_{2i} + \ldots\\
v_i &= \lambda v_{0i} + \xi v_{1i} + \xi^2 v_{2i} + \ldots\\
w_i &= \xi w_{1i} + \xi^2 w_{2i} + \ldots
\end{aligned} \tag{2.6}$$

Basing Eqs (2.1) and (2.3) one can present the membrane stress resultants in expanded form

$$\begin{aligned}
N_{xi} &= \lambda N_{xi0} + \xi N_{xi1} + \xi^2 N_{xi2} + \ldots\\
N_{yi} &= \lambda N_{yi0} + \xi N_{yi1} + \xi^2 N_{yi2} + \ldots\\
N_{xyi} &= \lambda N_{xyi0} + \xi N_{xyi1} + \xi^2 N_{xyi2} + \ldots
\end{aligned} \tag{2.7}$$

By substituting the expansion (2.6) into the equations of equilibrium (2.5), joint conditions and boundary conditions, the boundary-value problems of zero-, first- and second-order can be obtained. The zero approximation describes unmoved state while the first approximation represents the linear problem of stability and enables one to determine the eigenvalues, eigenvectors and critical speeds of the system. These equations can be reduced to a homogenous system of differential equilibrium equations. The second-order boundary-value problem can be reduced to a linear system of non-homogeneous equations the right-hand sides of which depend on the first-order displacements and load fields.

3. Solution to the problem

Below the linear analysis of moving orthotropic plate vibrations is presented. The web moves at constant speed c. One assumes that the plate is stretched only in its longitudinal direction, hence

$$N_{x0}(y) \neq 0 \qquad q = 0 \qquad N_{y0} = N_{xy0} = 0 \tag{3.1}$$

The inertial forces due to the in-plane displacements u and v are also neglected. Hence, for the linear problem the quantities u_1, v_1, N_{x1}, N_{y1}, N_{xy1} in Eqs (2.6) and (2.7) are negligible. The boundary conditions referring to the simple support of the plates at both ends are

$$w(x=0,y) = w(x=l,y) = 0 \qquad M_y(x=0,y) = M_y(x=l,y) = 0 \tag{3.2}$$

The zero-order solution of an orthotropic plate consisting of homogeneous fields which satisfies Eqs (3.1) is assumed as

$$u_0 = x\Delta \qquad v_0 = -\nu y\Delta \qquad N_{x0} = Eh\Delta \tag{3.3}$$

where Δ is the actual loading. This loading is specified as the product of a unit loading system and a scalar load factor Δ.

After taking into account Eqs (2.3), (3.1) and (3.3), the third differential equations appearing in Eqs (2.5) for the first-order approximation one can reduce to the form

$$\begin{aligned} &-\rho h(w_{1,tt} + 2cw_{1,xt} + c^2 w_{1,xx}) + N_{x0}w_{1,xx} - Dw_{1,xxxx} + \\ &-2(\nu\eta D + D_1)w_{1,xxyy} - \eta D w_{1,yyyy} = 0 \end{aligned} \tag{3.4}$$

The third dynamical component in Eq (3.4) plays a role similar to that of the compressive force loading a thin-walled plate in static stability problem (Kołakowski and Królak, 1995). In the second component of Eq (3.4) there are the derivatives with respect to x and t. Because of that one can not predict solution of Eq (3.4) in the x-direction in terms of modal forms. In further considerations the Galerkin-Bubnov orthogonalization procedure is used to find approximated solution of Eq (3.4). This solution has been determined in terms of a series of eigenfunctions for the unmoved plate (i.e. for $c = 0$)

$$w_1 = \sum_{m=1}^{K} W_{1m}(y) T_m(t) \sin \frac{m\pi x}{l} \tag{3.5}$$

where

$W_{1m}(y)$ – initially unknown function which will be determined using the transition matrix method (Unger, 1969)

$T_m(t)$ – unknown function of time.

To determine an unknown function $W_{1m}(y)$ in Eq (3.5) for unmoved plate one should assume $c = 0$. Numerical aspects of the problem being solved for the first-order fields demand introduction of the following orthogonal functions in the sense of boundary conditions for two longitudinal edges (Appendix C, Eqs (C.1))

$$\begin{aligned} f_{1m} &= w_1 \qquad f_{2m} = \frac{w_{1,y}}{b} = w_{1,\chi} \\ f_{3m} &= -\frac{M_y b^2}{\eta D} = w_{1,\chi\chi} + \nu w_{1,\zeta\zeta} \\ f_{4m} &= -\frac{12 Q_y^* b^3}{G h^3} = E_2(w_{1,\chi\chi} + \nu w_{1,\zeta\zeta})_{,\chi} + 4 w_{1,\zeta\zeta\chi} \end{aligned} \tag{3.6}$$

where

$$\zeta = \frac{x}{b} \qquad \chi = \frac{y}{b} \qquad E_1 = \frac{E}{G(1-\eta\nu^2)} \qquad E_2 = E_1\eta$$

After taking into account the new functions (3.6), the differential equilibrium equation (3.4) for $c = 0$ can be rewritten as follows

$$\begin{aligned} f_{2m} &= f_{1m,\chi} \\ f_{3m} &= f_{2m,\chi} + \nu f_{1m,\zeta\zeta} \\ f_{4m} &= E_2 f_{3m,\chi} + 4 f_{2m,\zeta\zeta} \end{aligned} \tag{3.7}$$

$$\frac{12b^2}{h^2}E_1\lambda\Delta(1-\eta\nu^2)f_{1m,\zeta\zeta}-E_1f_{1m,\zeta\zeta\zeta\zeta}-\nu E_2f_{2m,\zeta\zeta\chi}+$$

$$-f_{4m,\chi}-\frac{12\rho b^4}{Gh^2}f_{1m,tt}=0$$

The solutions of Eqs (3.7) may be formulated as follows

$$f_{jm}=F_{jm}(\chi)T_m(t)\sin\frac{m\pi b\zeta}{l}\qquad j=1,...,4 \tag{3.8}$$

The initially unknown functions F_{jm} (for the mth harmonic mode) will be defined using the numerical method of transition matrix. The system of ordinary modified differential equations (3.7) for the first-order approximation with appropriate join conditions for adjacent plates is solved using the transition matrices method (Unger, 1969; Kołakowski and Królak, 1995). The Runge-Kutta numerical integration of the equilibrium equations in the y-direction and the Godunov orthonalization method (Biderman, 1977) are used in order to obtain a relation between the state vectors on two longitudinal edges.

Let us return to the case of moving, orthotropic web for $c\neq 0$. Taking into account Eqs (3.5) and (3.6) the equilibrium equation (3.4) can be rewritten in the following form

$$\frac{12b^2}{h^2}E_1\lambda\Delta(1-\eta\nu^2)f_{1m,\zeta\zeta}-E_1f_{1m,\zeta\zeta\zeta\zeta}-\nu E_2f_{2m,\zeta\zeta\chi}+$$

$$-f_{4m,\chi}-\frac{12\rho b^2}{Gh^2}(b^2f_{1m,tt}+2cbf_{1m,t\zeta}+c^2f_{1m,\zeta\zeta})=0 \tag{3.9}$$

According to Eqs (3.5) and (3.6) the solutions of Eq (3.9) one can predict in the form

$$f_{jm}=\sum_{m=1}^{K}F_{jm}(\chi)T_m(t)\sin\frac{m\pi b\zeta}{l}\qquad j=1,...,4 \tag{3.10}$$

The functions F_{jm} in Eq (3.10) have been determined for the case $c=0$.

Since the trigonometric functions are incompatible in the $x(\zeta)$-direction, after substituting Eq (3.10) into Eq (3.9) the Galerkin-Bubnov orthogonalization method has been used

$$\sum_{i=1}^{J}\int_{S_i}X_i\delta w_i\,dS_i\equiv\sum_{i=1}^{J}\int_{S_i}X_i\delta f_{1i}\,dS_i=0 \tag{3.11}$$

where X_i is determined as the left-hand side of Eq (3.9) and integration is extended over the whole moving plate. In this way the set of K ordinary differential equations with respect to the function $T_m(t)$ can be determined in the following form

$$\frac{d^2T_m}{dt^2}a_{2m} + T_m a_{0m} + \sum_{n=1}^{K} \frac{dT_n}{dt} a_{1mn} = 0 \qquad m = 1, 2, ..., K \tag{3.12}$$

The coefficients of the set (3.12) are given in Appendix D. Basing of Eq (3.12) one can determine eigenvalues and eigenvectors of the system.

4. Numerical results and discussion

Above, it was assumed that the moving plate is stretched at a uniform rate in the axial direction and the stiffness of the rolls support structure is not taken into account. When the stiffness is considered, the in-plane axial tension of the web is (cf Mote, 1965)

$$N_{x0} = N_{x0}^{*} - \kappa\rho hc^2 = Eh\Delta - \kappa\rho hc^2 \tag{4.1}$$

In this case Eq (3.3) one should modify to the form

$$u_0 = x\Delta - \kappa\rho c^2 \frac{1-\eta\nu^2}{E} x \qquad v_0 = -\nu y\Delta \tag{4.2}$$

This crosswise boundary condition modification involves also the change in equilibrium equations. Thus, in Eqs (3.7) and (3.9) one should add the following component

$$\kappa c^2 f_{1m,\zeta\zeta} \tag{4.3}$$

After taking into account Eq (4.1) one can obtain the axial tension expression

$$R = \sum_{i=1}^{J} \int_0^{b_i} N_{xi0}(y)\, dy_i = R_0 + \rho hb_i c^2(1-\kappa) \tag{4.4}$$

where $0 \leqslant \kappa \leqslant 1$.

For the rolls support stiffness $\kappa = 0$, the rolls are free to move relative to each other under tension variation. For $\kappa = 1$, the two rolls are rigidly fixed with respect to each other, eliminating the plate tension increase with

the axial transport speed c. For $0 < \kappa < 1$, the rolls support system has finite stiffness and the axial tension decreases with c.

Numerical investigations have been carried out for five approximating functions ($K = 5$) and for two different materials of the web: steel and paper. The parameter values are given in Table 1.

Table 1. Numerical data

Material	Steel plate I	Steel plate II	Paper web
l [m]	1.5	1.0	1.194
b [m]	0.5	0.2	0.597
h [m]	$3 \cdot 10^{-3}$	$4.047 \cdot 10^{-3}$	$0.3 \cdot 10^{-3}$
ρ [kg/m^3]	7800	7800	133.33 (0.04 kg/m^2)
R_0 [N]	$30 \cdot 10^3$	$2.428 \cdot 10^3$	32.835
E [N/m^2]	$0.2 \cdot 10^{12}$	$0.2 \cdot 10^{12}$	$5 \cdot 10^9$
ν [-]	0.3	0.3	0.3

The parameters of the steel plate I characterise the saw band blades investigated (Ulsoy and Mote, 1982). A comparison of the lowest transverse and the lowest torsional natural frequencies of the steel web I versus axial velocity for the obtained and published results is given in Fig.3. The compared results are in excellent agreement.

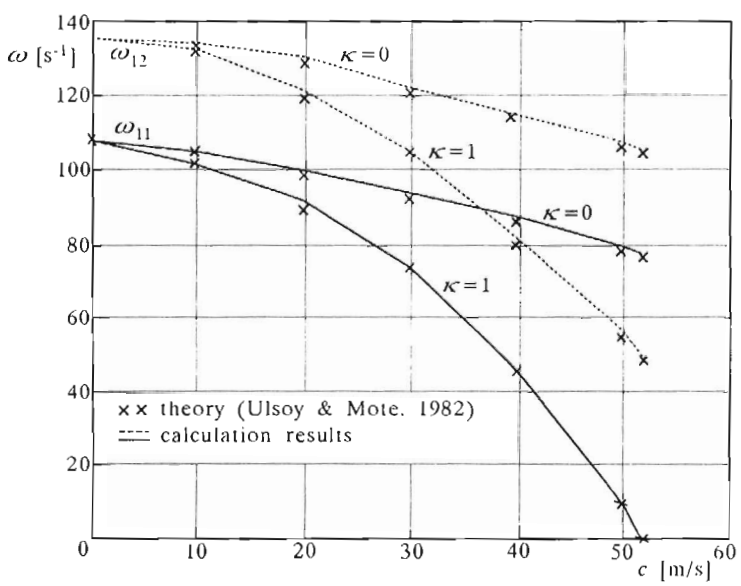

Fig. 3. Comparison of the lowest transverse ω_{11} and the lowest torsional ω_{12} natural frequencies of the steel plate I

The dynamic behaviour of the steel plate II was investigated. The parameter values of the plate are given in Table 1. In Table 2 there are orthotropic material properties which were assumed. The values of ratios E_y/E, G/E and ν are assumed after Chandra and Raju (1973).

Table 2. Elastic constants for various cases of orthotropic plate material

E [MPa]	E_y [MPa]	G [MPa]	$\eta = E_y/E$	G/E	ν
$0.606 \cdot 10^5$	$0.2 \cdot 10^6$	$0.735 \cdot 10^4$	0.3031	0.1213	0.3
$1.013 \cdot 10^5$	$0.2 \cdot 10^6$	$2.019 \cdot 10^4$	0.5064	0.1994	0.3
$1.408 \cdot 10^5$	$0.2 \cdot 10^6$	$3.975 \cdot 10^4$	0.7041	0.2823	0.3
$1.672 \cdot 10^5$	$0.2 \cdot 10^6$	$5.424 \cdot 10^4$	0.8358	0.3245	0.3
$0.2 \cdot 10^6$	$0.2 \cdot 10^6$	$7.692 \cdot 10^4$	1.0	0.3846	0.3
$0.2 \cdot 10^6$	$2.393 \cdot 10^5$	$7.764 \cdot 10^4$	1.1964	0.3846	0.25074
$0.2 \cdot 10^6$	$2.84 \cdot 10^5$	$8.018 \cdot 10^4$	1.4202	0.4009	0.21123
$0.2 \cdot 10^6$	$3.949 \cdot 10^5$	$7.874 \cdot 10^4$	1.9747	0.3937	0.15192
$0.2 \cdot 10^6$	$6.598 \cdot 10^5$	$8.004 \cdot 10^4$	3.2992	0.4002	0.12006

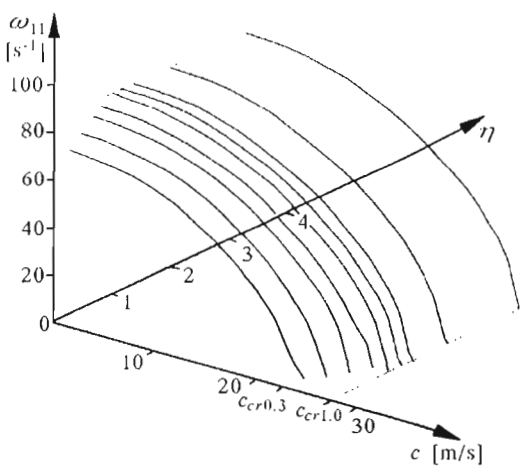

Fig. 4. Lowest transverse natural frequency for various orthotropy factors of the steel plate II ($\kappa = 1$)

First, the lowest transverse natural frequencies for various values of the orthotropy factor η and the axial transport speed c were calculated. The results are presented in Fig.4. In this case, for a constant axial tension of the plate, the lowest transverse natural frequency ω_{11} decreases with the increasing axial velocity at a rate dependent on the orthotropy factor value. In all the investigated ranges of η, a velocity exists at which the fundamental

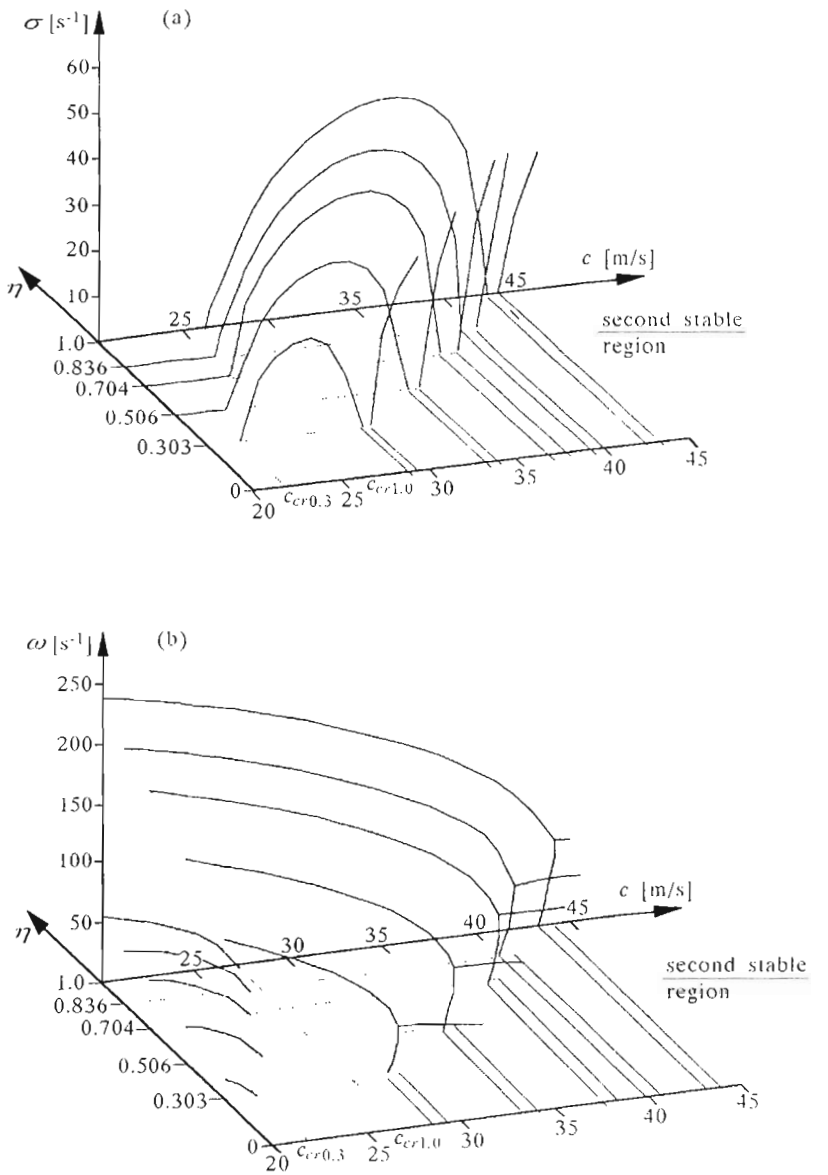

Fig. 5. Lowest eigenvalues for various orthotropy factors of the steel plate II at supercritical transport speeds, (a) real port, (b) imaginery parts

natural frequency vanishes indicating the divergence instability of the system. In the range $\eta < 1$ the orthotropy factor when decreasing diminishes the critical axial speed c_{cr}. In the range of the orthotropy factor $1.0 \leqslant \eta \leqslant 3.3$ significant differences in changes of natural frequencies values have not been observed.

Dynamic behaviour of the steel plate II was investigated above the critical transport speed. Let σ and ω denote the real and imaginary parts of eigenvalues, respectively. Non-zero σ indicates the instability of the system and ω is the natural frequency of the plate. At a supercritical transport speed, at first, the plate experiences the divergent instability (the fundamental mode with non-zero σ and zero ω (Fig.5) and next the flutter instability (non-zero σ and non-zero ω). Between those two states there is the second stable region where $\sigma = 0$. The change in the orthotropy factor value in the range $0.303 \leqslant \eta \leqslant 1.0$ changes the second stable region location as it is shown in Fig.5.

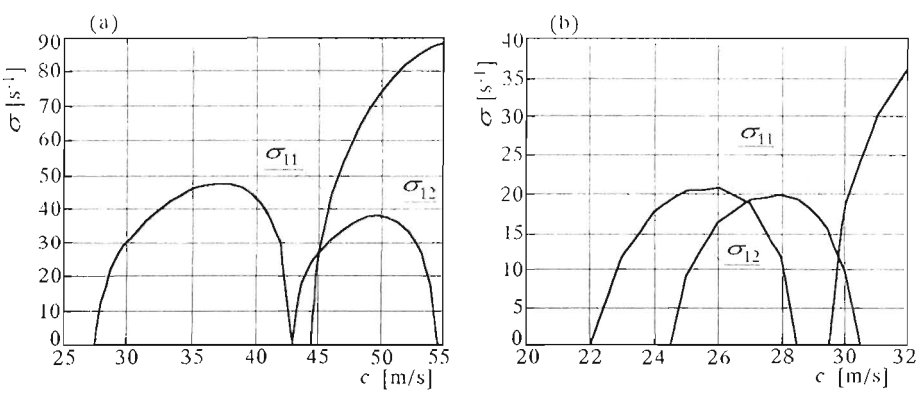

Fig. 6. Real parts of lowest transverse σ_{11} and torsional σ_{12} eigenvalues of the steel plate II, (a) $l/b = 1.3$, $\eta = 1$, $\kappa = 1$; (b) $l/b = 1.3$, $\eta = 0.303$, $\kappa = 1$

Apearence of the second stable region depends on the slenderness ratio l/b and the orthotropy factor of the plate. The plots of the real part of eigenvalues versus axial transport speed of the steel plate II with $l/b = 1.3$ for izotropic ($\eta = 1$) and orthotropic ($\eta = 0.303$) cases are shown in Fig.6a and Fig.6b, respectively. There are no second stable regions at supercritical transport speed. For the izotropic plate the second stable region does not exist for the slenderness ratio $l/b < 1.3$. Below this minimum value of the slenderness ratio the lowest torsional eigenvalue with the real part $\sigma_{12} > 0$ apears at lower axial velocities. When the orthotropy factor of the plate dimnishes the

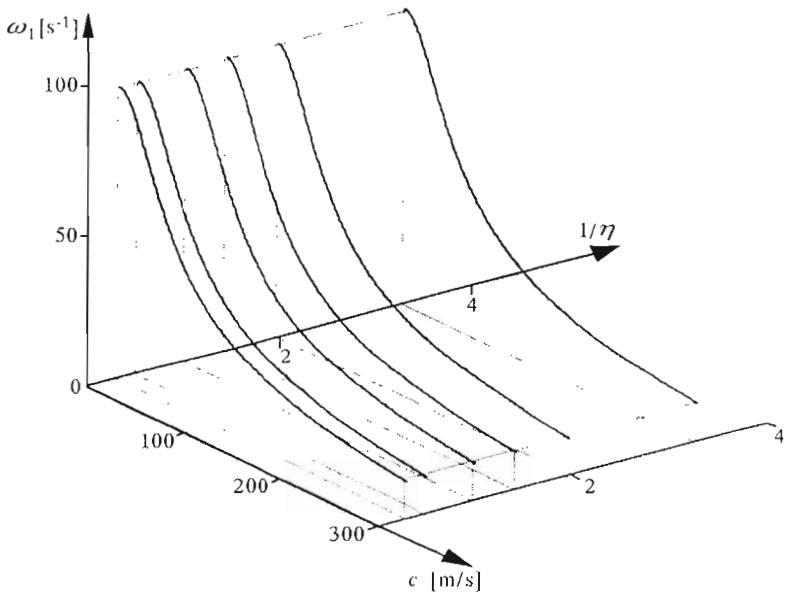

Fig. 7. Lowest transverse natural frequency for various orthotropy factors of the paper web ($\kappa = 0$)

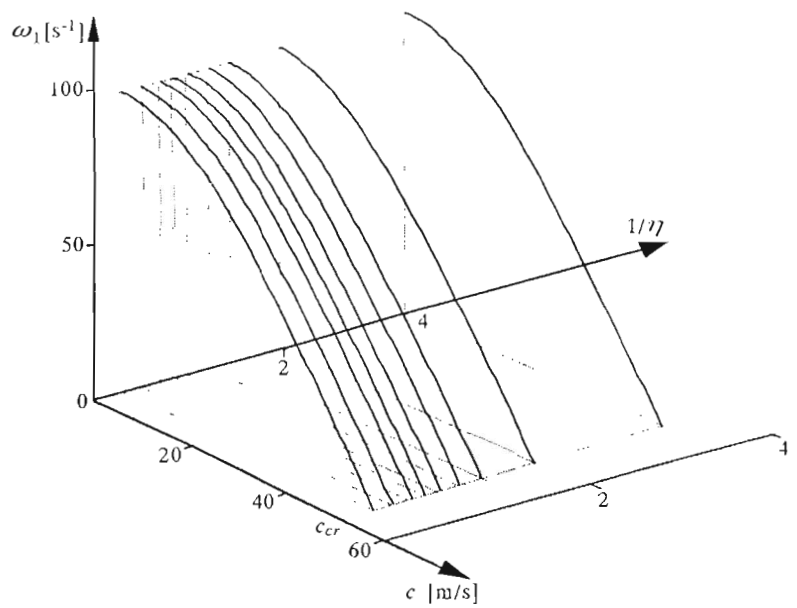

Fig. 8. Lowest transverse natural frequency for various orthotropy factors of the paper web ($\kappa = 0.5$)

minimum slenderness ratio increases. It is illustrated in Fig.6b for $l/b = 1.3$ and $\eta = 0.303$.

Furthermore, the dynamic behaviour of a thin paper web was investigated. Parameter values of the web are given in Table 1. Equilibrium displacement and stress distribution of the same paper web were investigated by Lin and Mote (1995). The dimensionless ratios E_y/E, G/E and ν take the values from Table 2.

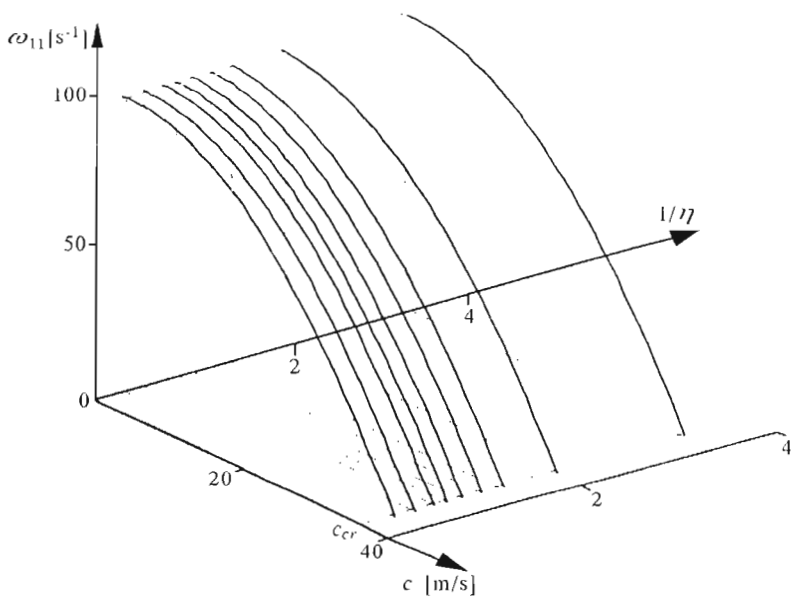

Fig. 9. Lowest transverse natural frequency for various orthotropy factors of the paper web ($\kappa = 1.0$)

The lowest transverse natural frequencies ω_{11} for various values of the orthotropy factor $1/\eta$, rolls support stiffness κ and axial transport speed c were calculated. The results are presented in Fig.7, Fig.8 and Fig.9 for $\kappa = 0$, $\kappa = 0.5$ and $\kappa = 1$, respectively. In all these cases, for the constant axial tension of the web $R_0 = 32.835\,\mathrm{N}$ (i.e. $N^*_{x0} = 55\,\mathrm{N/m}$), the lowest transverse natural frequency decreases with the increasing axial velocity at a rate depending on the value of κ. For $\kappa > 0$ a velocity exists at which the fundamental natural frequency vanishes indicating the divergence instability of the system. In the considered range of the orthotropy factor $1/\eta$ significant differences in changes of natural frequencies values have not been observed.

5. Conclusions

In the paper a new method of dynamic analysis of axialy moving orthotropic plate is presented. The differential equations of motion are derived from Hamilton's principle taking into account the Lagrange description, Green's strain tensor for thin-walled plates and Kirchhoff's stress tensor.

Results of numerical investigations show the solution to a linear problem. In investigations the effect of the orthotropy factor, the axial transport velocity and the rolls support system on natural frequencies and stability of the plate motion are presented. At undercritical transport speeds for both the steel plate and paper web the lowest transverse and torsional natural frequencies decrease with the increasing axial velocity at a rate depending mainly on the rolls support stiffness. A decrease of the steel plate orthotropy factor in the range $\eta < 1$ dimnishes the critical axial speed of the plate.

The plate may experience the divergent or flutter instability at supercritical transport speeds. The second stable region above the critical speed may exist. This raises the posibility of stable operations at speeds higher than the critical one. Apearence of the second stable region depends on the slenderness ratio and the orthotropy factor of the plate.

In the case of the considered paper web a strong influence of rolls support system on natural frequencies and critical transport velocity values has been detected. In the considered range of the web orthotropy factor value no significant differences in changes of eigenvalues have been observed.

A. Appendix

The case of the body motion within the time interval (t_0, t_1) was taken into considerations in the Lagrange description. In the time interval between the initial and final positions one takes into account different trajectories of motion the system points. Actual trajectories differ from those satisfying Hamilton's principle

$$\delta \int_{t_0}^{t_1} L \, dt = 0 \tag{A.1}$$

where

L – Lagrange function, $L = U - V + W$

U – kinetic energy of the system

V – potential energy of the system, $V = V_b + V_m$
V_b – elastic strain energy of bending
V_m – elastic strain energy of membrane state deformation
W – work of the external forces.

The above quantities for the ith plate can be expressed as follows

$$
\begin{aligned}
U_i &= \frac{1}{2}\rho_i h_i \int\limits_{S_i} \left[(c + u_{i,t} + cu_{i,x})^2 + (v_{i,t} + cv_{i,x})^2 + (w_{i,t} + cw_{i,x})^2\right] dS_i \\
V_{mi} &= \frac{1}{2} \int\limits_{S_i} \left(N_{xi}\varepsilon_{xi} + N_{yi}\varepsilon_{yi} + N_{xyi}\gamma_{xyi}\right) dS_i \\
V_{bi} &= \frac{1}{2} \int\limits_{S_i} \left(M_{xi}\kappa_{xi} + M_{yi}\kappa_{yi} + 2M_{xyi}\kappa_{xyi}\right) dS_i \qquad \text{(A.2)} \\
W_i &= \int\limits_0^{b_i} N_{xi0}(y_i)\Big|_{x=0}[u(l) - u(0)]\, dy_i + \\
&+ \int\limits_0^{l} N_{yi0}(x_i)\Big|_{y=0}[v(b_i) - v(0)]\, dx_i + \int\limits_0^{b_i} N_{xyi0}(y_i)\Big|_{x=0}[u(l) - u(0)]\, dy_i + \\
&+ \int\limits_0^{l} N_{xyi0}(x_i)\Big|_{y=0}[v(b_i) - v(0)]\, dx_i + \int\limits_{S_i} q_i w_i\, dS_i
\end{aligned}
$$

where S_i – surface of the ith plate.

B. Appendix

The kinematics and static continuity conditions at the joint of the adjacent plates (Fig.2)

$$
\begin{aligned}
&u_{i+1}\Big|^0 = u_i\Big|^+ && w_{i+1}\Big|^0 = w_i\Big|^+ \\
&v_{i+1}\Big|^0 = v_i\Big|^+ && w_{i+1,y}\Big|^0 = w_{i,y}\Big|^+ \\
&M_{y(i+1)}\Big|^0 - M_{yi}\Big|^+ = 0 && N^*_{y(i+1)}\Big|^0 - N^*_{yi}\Big|^+ = 0 \\
&Q^*_{y(i+1)}\Big|^0 - Q^*_{yi}\Big|^+ = 0 && N^*_{xy(i+1)}\Big|^0 - N^*_{xyi}\Big|^+ = 0
\end{aligned}
\qquad \text{(B.1)}
$$

where the internal cross-section forces are

$$
\begin{aligned}
N^*_{yi} &= N_{yi} - \rho_i h_i (c v_{i,t} + c^2 v_{i,x}) \\
N^*_{xyi} &= N_{xyi} - \rho_i h_i (c^2 + c u_{i,t} + c^2 u_{i,x}) \\
Q^*_{yi} &= N_{yi} w_{i,y} + N_{xyi} w_{i,x} - \eta_i D_i w_{i,yyy} + \\
&- (\nu_i \eta_i D_i + 2 D_{1i}) w_{i,xxy} - \rho_i h_i (c w_{i,t} + c^2 w_{i,x})
\end{aligned} \tag{B.2}
$$

The superscripts "0" in (B.2) denote the edge $y_i = b_i$ of the ith plate, the superscipts "+" denote the edge $y_{i+1} = 0$ of the $(i+1)$st plate.

C. Appendix

Taking into account Eqs (3.1) and Eqs (2.7) for $c = 0$ the conditions resulting from Hamilton's principle for two longitudinal edges have been derived. On the edges the relation between the state vectors is derived using the modified transition matrices method

$$
\begin{aligned}
&\int N^*_{yi} \delta v_i \, dx_i = 0 \qquad && \int N^*_{xyi} \delta u_i \, dx_i = 0 \\
&\int M_{yi} \delta w_{i,y} \, dx_i = 0 \qquad && \int Q^*_{yi} \delta w_i \, dx_i = 0
\end{aligned} \tag{C.1}
$$

For the first-order approximation the coupling between the membrane state and the bending state appears when the co-operation conditions of two component plates are satisfied. For the unloaded and immovable state the flat plate surface has been assumed and it is sufficient to take only the two last relations of Eq $(C.1)_{3,4}$ for the first-order approximation.

D. Appendix

The coefficients of Eqs (3.12) are given in the following form

$$
a_{2m} = \sum_{i=1}^{J} \Big(-\frac{6 b_i^3 \rho_i}{G_i h_i^2} l \int_0^1 F^2_{1m}(\chi_i) \, d\chi_i \Big)
$$

$$a_{1mn} = \sum_{i=1}^{J}\Big[-\frac{12b_i^2\rho_i}{G_i h_i^2}2cl\int_0^1 F_{1m}(\chi_i)F_{1n}(\chi_i)\frac{n\pi b_i}{l}\alpha_{nm}\,d\chi_i\Big] \qquad (D.1)$$

$$a_{0m} = \sum_{i=1}^{J}\Big\{\int_0^1 F_{1m}^2(\chi_i)l\frac{6b_i\rho_i}{G_i h_i^2}\Big[c^2\Big(\frac{m\pi b_i}{l}\Big)^2 - b_i^2\omega_m^2\Big]\,d\chi_i\Big\}$$

where

$$\alpha_{nm} = \begin{cases} 0 & \text{for} \quad n^2 = m^2 \\ \dfrac{m}{\pi(m^2-n^2)}[1-(-1)^{n+m}] & \text{for} \quad n^2 \neq m^2 \end{cases} \qquad (D.2)$$

Acknowledgement

This paper was supported by the State for Scientific Research (KBN) under grant 7 T08E 028 12.

References

1. BIDERMAN B.L., 1977, *Mechanics of Thin-Walled Structures. Statics*, (in Russian), Mashinostroenie, Moscow

2. CHANDRA R., RAJU B.B., 1973, Postbuckling Analysis of Rectangular Orthotropic Plates, *Int. Journal of Mechenical Science*, **16**, 81-97

3. KOŁAKOWSKI Z., KRÓLAK M., 1995, Interactive Elastic Buckling of Thin-Walled Closed Orthotropic Beam-Columns, *Engineering Transactions*, **43**, 4, 571-590

4. LIN C.C., MOTE C.D., JR., 1995, Equilibrium Displacement and Stress Distribution in a Two Dimensional, Axially Moving Web under Transverse Loading, *Journal of Applied Mechanics ASME*, **62**, 772-779

5. LIN C.C., MOTE C.D., JR., 1996, The Wrinkling of Thin, Flat, Rectangular Webs, *Journal of Applied Mechanics ASME*, **63**, 774-779

6. LIN C.C., 1997, Stability and Vibration Characteristics of Axially Moving Plates, *Int. Journal Solid Structures*, **34**, 24, 3179-3190

7. MOTE C.D., JR., 1965, A Study of Band Saw Vibrations, *Journal of the Franklin Institute*, **279**, 6, 430-444

8. ULSOY A.G., MOTE C.D., JR., 1982, Vibration of Wide Band Saw Blades, *Journal of Engineering for Industry ASME*, **104**, 1, 71-78

9. UNGER B., 1969, Elastisches Kippen von beliebig gelagerten und aufgehaengten Durchl auftraegern mit einfachsymmetrischen, in *Traegerachse veraenderlichem Querschnitt und einer Abwandlung des Reduktionsverffahrens als Loesungsmethode*, Dissertation D17, Darmstadt

10. WICKERT J.A., MOTE C.D., JR., 1988, Current Research on the Vibration and Stability of Axially Moving Materials, *Shock and Vibration Digest*, **20**, 3-13

11. WICKERT J.A., MOTE C.D., JR., 1990, Classical Vibration Analysis of Axially-Moving Continua, *Journal of Applied Mechanics ASME*, **57**, 738-744

Zachowanie dynamiczne poruszającej się osiowo cienkiej ortotropowej płyty

Streszczenie

W pracy przedstawiono nową metodę analizy dynamicznej poruszających się osiowo płyt ortotropowych. Wyniki obliczeń numerycznych pokazują rozwiązanie problemu liniowego. Badano wpływ współczynnika ortotropii, prędkości osiowej oraz sztywności podparcia rolek na poprzeczne i skrętne częstości drgań własnych i stateczność ruchu płyty. Wartości najniższych częstości własnych zmniejszają się ze wzrostem prędkości w podkrytycznym zakresie prędkości przesuwu. W zakresie nadkrytycznym może występować niestateczność dywergencyjna lub typu flater. W zakresie nadkrytycznym może się również pojawić drugi obszar stateczności ruchu.

Manuscript received April 20, 1998; accepted for print September 10, 1998